*Catalysis Letters, Vol. 116, Nos. 3–4, August 2007 (© 2007)*
DOI: 10.1007/s10562-007-9111-z


# Low-temperature water-gas shift reaction on $Au/CeO_2$ catalysts – the influence of catalyst pre-treatment on the activity and deactivation in idealized reformate

A. Karpenko,[a] Y. Denkwitz,[a] V. Plzak,[b] J. Cai,[a] R. Leppelt,[a] B. Schumacher,[a] and R. J. Behm[a,*]

[a]*Institute of Surface Chemistry and Catalysis, Ulm University, D-89069 Ulm, Germany*
[b]*Centre for Solar Energy and Hydrogen Research, Helmholtzstr. 8, D-89081 Ulm, Germany*

Received 27 March 2007; accepted 31 March 2007

The effect of the pre-treatment temperature and atmosphere on the surface composition and on the activity and stability of well defined $Au/CeO_2$ catalysts in the low-temperature water-gas shift reaction in dilute water gas was investigated by X-ray photoelectron spectroscopy, kinetic measurements and *in-situ* IR spectroscopic (DRIFTS) measurements, comparing different reductive and oxidative conditioning procedures. Reductive conditioning at 200 °C yields the most active catalyst. Physical origin and consequences of the resulting differences in the reaction behavior are discussed.

**KEY WORDS:** water-gas shift reaction; Au catalyst; catalyst conditioning; deactivation; $Au/CeO_2$; GC; DRIFTS; XPS.

## 1. Introduction

In the recent decades oxide supported gold catalysts have attracted increasing interest as highly active catalysts for a number of oxidation and reduction reactions, including also the water-gas shift (WGS) reaction [1–4]. The latter reaction is particularly attractive due to its possible application for CO removal from CO contaminated $H_2$-rich feed gases for Polymer Electrolyte Fuel Cells (PEFCs), as they are produced by partial oxidation and/or steam reforming of fossil fuels or biomass derived fuels [5,6]. High WGS activities reaction have been reported for $Au/ZrO_2$ [7], $Au/Co_3O_4$ [8], $Au/TiO_2$ [9,10], $Au/Fe_2O_3$ [11–14] and $Au/CeO_2$ [3,14–20] catalysts, with the activity decreasing in the order $Au/Fe_2O_3 \cong Au/TiO_2 \cong Au/ZrO_2 > Au/Co_3O_4$ [3]. It is tempting and plausible to assume a similar reaction mechanism for these catalysts; a comprehensive and more quantitative understanding of the reaction on these catalysts is hindered, however, by the widely varying procedures and parameters for catalysts synthesis and catalyst pre-treatment ('activation'), and also by the very different reaction conditions.

This is topic of the present paper, where we report on the effect of the catalyst pre-treatment, specifically the procedure and parameters of the activation process, on the activity, deactivation and reaction/deactivation behavior of $Au/CeO_2$ catalysts in the WGS reaction. We will apply different oxidative, reductive or thermal activation procedures on the same raw catalyst precursor. This report is part of an extensive study on the WGS reaction on $Au/CeO_2$ catalysts, which were prepared by a deposition-precipitation method [21,22]. First results on the kinetics and mechanism of the reaction and on the effects of catalyst loading for reaction in idealized gas mixtures have been reported recently in ref. [23], results on the effect of increasing $CO_2$ and $H_2$ contents and on the influence of the surface area of the support on the activity and in particular on the deactivation behavior were presented in refs. [24] and [25], respectively.

In previous studies three different general procedures have been applied for the activation of $Au/CeO_2$ catalysts: reductive pre-treatment, calcination or thermal treatment in an inert atmosphere. In most cases reductive pre-treatment in $H_2$ (1–10% $H_2$ in inert gas as balance at different temperatures) was used to activate $Au/CeO_2$ catalysts for the WGS reaction [18,26–28]. Reductive pre-treatment with CO was also investigated [27]. Since we wanted to avoid a possible blocking of active sites with carbonates and formates, whose generation could be observed in the presence of CO with DRIFTS [24], we did not test CO as reducing agent. Another possible conditioning procedure is calcination, which has also been reported for $Au/CeO_2$ catalysts [12,14,15,19,28]. It should be noted that in some cases the measurement temperatures exceeded the conditioning temperatures [14,26,28], which can lead to further catalyst modification during the reaction. Thermal treatment in inert atmosphere was chosen as one conditioning procedure, since several groups reported a

*To whom correspondence should be addressed.
E-mail: juergen.behm@uni-ulm.de

higher activity of Au/α-$Fe_2O_3$ catalysts for the room temperature CO oxidation, if the precipitate was not treated at higher temperatures [29–31]. Since in our measurements the WGS reaction is performed at 180 °C, the samples had to be conditioned at higher temperature in order to reduce activation effects induced by the reaction. Therefore, we investigated the effect of reductive, thermal and oxidative treatment in the temperature range between 200 and 400 °C, measuring the initial activity and following the subsequent deactivation in idealized reformate (dilute water gas). These kinetic measurements were complemented by *in-situ* IR spectroscopic measurements performed in a diffuse reflectance FTIR spectroscopy (DRIFTS) set-up, which allowed us to characterize the initial state of the catalysts after conditioning and the further accumulation of adsorbed reaction intermediates and side products during reaction in idealized reformate under similar conditions as in the kinetic measurements. In addition, we characterized the catalyst surface composition at different stages by X-ray photoelectron spectroscopy (XPS) and by thermal desorption spectroscopy (TPD).

## 2. Experimental

### 2.1. Catalyst preparation

The catalysts were prepared by a deposition-precipitation procedure, using commercial CeO2 powder as support (HSA 15 from Rhodia, calcined in air at 400 °C) and $HAuCl_4 \cdot 4H_2O$ for deposition of Au. Further details are given in refs. [21,22]. The Au metal content was determined via inductively coupled plasma atom emission spectroscopy (ICP-AES). All measurements were performed with catalysts having a BET surface of 188 $m^2\ g^{-1}$ and 2.7 wt.% Au loading. Details of the conditioning procedures are described in section 3.1.

### 2.2. Catalyst characterization

The chemical composition of the catalysts was characterized by X-ray photoelectron spectroscopy (XPS, PHI 5800 ESCA system), using monochromatized $AlK_\alpha$ radiation. The survey spectra were measured in the range between 0 and 1400 eV binding energy (BE). Detail spectra of gold (Au(4f)) and ceria (Ce(3d)) were measured in the range from 75 to 100 eV and from 875 to 925 eV (0.125 eV and 20 ms per step), respectively. In order to remove surface charging effects, the BEs were calibrated using the $Ce^{4+}(3d^{10}4f\ ^0V^n)$ ($u'''$) signal at 916.6 eV as reference [23,32]. The intensity scales of the Au(4f) and O(1s) detail spectra were normalized to constant Ce(3d) intensity. Fits of the Au(4f) peaks were performed based on the following assumptions: (i) the difference between $Au(4f_{7/2})$ and $Au(4f_{5/2})$ was fixed at 3.7 eV, (ii) the integral intensity of the $Au(4f_{5/2})$ peak is 3/4 of that of the $Au(4f_{7/2})$ peak, and (iii) the peak widths (FWHM) for both peaks are equal [33]. Furthermore, the Lorenz–Gauss ratio for each Au species was kept constant. The Ce(3d) region consist of five Ce(3d) peaks (three peaks resulting from $CeO_2$ and two peaks resulting from $Ce_2O_3$), and the fits are based on the following assumption: (i) the difference between $Ce(3d_{3/2})$ and $Ce(3d_{5/2})$ is 18.5 eV, (ii) the integral intensity of the $Ce(3d_{3/2})$ signal is 2/3; of the $Ce(3d_{5/2})$ signal, (iii) the peak widths (FWHM) for both signals of one peak are equal, (iv) the peak widths of the $v(Ce^{4+})$, $v'''$ $(Ce^{4+})$ and $v_0(Ce^{3+})$ peaks are equal, (v) the peak width of $v'(Ce^{3+})$ is 1.56 of that of the v peak and (vi) the width of the $v''(Ce^{4+})$ is 1.71 of that of the v peak (see [23] and references therein). The $Ce^{3+}$ concentration in ceria is determined via the following equation [32,34]:

$$c_{Ce^{3+}} = \frac{I(v_0) + I(v') + I(u^0) + I(u')}{\sum_i ((Iu^i) + I(v^i))}$$

For XPS measurements, catalyst conditioning was performed *ex-situ*.

### 2.3. Activity measurements

Activity measurements were performed in a quartz tube micro reactor (i.d. 4 mm) located in a ceramic tube oven with typically 75 mg powder (catalyst:α-$Al_2O_3$ = 1:20). The reaction was carried out in idealized reformate (dilute water gas, 1 kPa CO, balance $N_2$ (dry) 2 kPa $H_2O$, 60 N ml $min^{-1}$). In order to obtain differential conversions, the catalyst samples were diluted with α-$Al_2O_3$ which is not active for the reaction in the studied temperature range (reaction temperature 180 °C). Water was added to the gas stream using a saturation unit. The influent and effluent gas was analyzed by on-line gas chromatography (DANI, GC 86.10) with $H_2$ as carrier gas. High purity gases from Westphalen (CO 4.7, $N_2$ 6.0, $H_2$ 5.0) were used. Evaluation of the Weisz criterion showed the absence of mass-transport-related problems [35]. More details on the kinetic measurements are given elsewhere [36].

### 2.4. Infrared investigations

*In-situ* IR investigations were performed in a DRIFTS (diffuse reflectance infrared Fourier transform spectroscopy) configuration with a Magna 560 spectrometer form Nicolet, equipped with a liquid $N_2$ cooled MCT narrow band detector and a commercial *in-situ* reaction cell unit from Harricks (HV-DR2). This set-up allows measurement in a continuous flow of gas mixtures, equal to those used in the activity measurements, and at elevated temperatures. Typically, 400 scans (acquisition time 3 min) at a nominal resolution of 8 $cm^{-1}$ were added for one spectrum. The IR data were

evaluated as Kubelka-Munk units, which are linearly related to the adsorbate concentration [37]. To analyze the product gas flow, a gas chromatograph (Chrompack CP 9001) was connected to the exhaust of the DRIFTS cell. For further details see ref. [38].

## 3. Results and discussion

### 3.1. Effect of the catalyst pre-treatment on the catalyst composition

The surface composition of the untreated, raw Au/$CeO_2$ catalyst as well as that of differently pre-treated samples, after calcination at 200 °C (sample code '*O200*') or 400 °C ('*O400*'), or after reductive conditioning at the respective temperatures ('*H200*', '*H400*'), or after drying in inert atmosphere ($N_2$) ('*N200*'), was characterized by XPS, DRIFTS and TPD. For conditioning, the catalyst was first heated in $N_2$ to the respective temperature, then kept at that temperature for 30 min in an $N_2$ flow, and subsequently exposed to the respective conditioning atmosphere for 45 min (reductive and inert conditioning) or 30 min (oxidative conditioning), respectively. Afterwards it was kept for another 30 min at the conditioning temperature in an $N_2$ stream and then cooled down to the reaction temperature in $N_2$.

#### 3.1.1. XPS results

The main XPS results are listed in table 1, Au(4f) detail spectra are shown in figure 1 (upper left panel). The spectrum of the untreated catalyst (figure 1a) shows a broad peak with a maximum at about 84.8 eV, i.e., it is shifted to higher BEs compared to metallic gold (84.0 eV [39,40]). This behavior agrees closely with previous reports on untreated Au/$CeO_2$ catalysts prepared via deposition-precipitation [23,28]. A formal evaluation of the $Au^0$ content, assuming a BE of 84.0 eV and a FWHM of ~2 eV (see section 2), would result in value of 40.2%. Considering, however, that final-state relaxation effects can lead to a considerable shift of the Au(4f) BE to higher energies for the very small particles expected for this catalyst, the above value for the $Au^0$ content has to be used as lower limit.

After calcination at 200 °C, the spectrum exhibits a wide peak with two weak maxima at about 84.6 and 87.9 eV (figure 1, curve b). The lower (Ce(3d) normalized) intensity of this and the following spectra compared to that in curve a is explained by the decreasing absorption of Ce(3d) intensity due to the more pronounced formation of Au particles. The onset at low BEs is slightly lower than 82 eV, it ends at about 92 eV. As shown in the fit to this curve, the absence of a distinct minimum can be explained by a higher contribution from $Au^{3+}$ (85.8 eV [41]). Also in this case, particle size effects cannot be fully excluded, and therefore the formal $Au^0$ content of 47% should be used as a lower limit. After calcination at 400 °C (figure 1, curve c), the increasing Au particle size allows a more reliable fit of the Au(4f) peak by contributions of $Au^0$ and $Au^{3+}$, as described in section 2.2. (Note that the $Au^0$ particle sizes are still below the resolution limit of XRD.) Now the content of metallic gold amounts to ~76%. Similar observations of largely metallic Au species after calcination of a Au/$CeO_2$ catalyst at 400 °C (calcination in air, 10 h) were reported also by Fu *et al.* [42].

Reductive conditioning in 10% $H_2/N_2$ leads to significantly stronger reduction and $Au^0$ formation than calcination. Reductive treatment at 200 °C (figure 1, curve d) and 400 °C (figure 1, curve e) results in Au(4f) peaks with a clear maximum at 83.9 eV. Fitting with $Au^0$ and $Au^{3+}$ signals yields $Au^0$ contents of 80.3% and 90.3%, respectively. Similar to calcination, the higher conditioning temperature leads to a stronger reduction (oxide decomposition).

In total, reductive conditioning is more efficient in obtaining metallic Au species than calcination under otherwise similar conditions because of the combination of chemical reduction and thermal composition in $H_2$ containing atmosphere, while in oxidative atmosphere these effects are counteracting. The incomplete reduction after the *H400* pre-treatment may be related to diffusion of $Au^{n+}$ into the ceria support during the heating step in the preparation process, as had been suggested by Fu *et al.* [19], or it results from $Au^{n+}$ species at the interface between Au and support [2].

XPS data of the Ce(3d) region of the untreated Au/$CeO_2$ catalyst and of the differently pre-treated samples (*O200*, *O400*, *H200*, and *H400*) are presented in the bottom panel in figure 1; the resulting $Ce^{3+}/Ce$ ratios and the $I_{Au(4f)}/I_{Ce(3)}$ intensity ratios are collected in table 1. As described in the experimental part and in ref. [23], the Ce(3d) region includes a number of peaks, which result from different electronic states of $Ce^{4+}$ and $Ce^{3+}$. The relative intensity of the $Ce^{3+}$ related peaks, normalized to the total Ce(3d) intensity, increased upon

Table 1
Surface composition of a 2.7 wt.% Au/$CeO_2$ catalyst after different conditioning procedures as described in the text

| Pre-treatment | *RT* | *H200* | *H400* | *O200* | *O400* |
|---|---|---|---|---|---|
| $Au^{n+}/Au$ (%) | 59.8 | 19.7 | 9.7 | 53.5 | 24.3 |
| $Ce^{3+}/Ce$ (%) | 18.0 | 20.9 | 29.6 | 14.0 | 20.4 |
| $I_{Au(4f)}/I_{Ce(3d)}$ | 0.21 | 0.096 | 0.096 | 0.15 | 0.11 |
| BE($Au^0(4f_{7/2})$) (eV) | 84.3 | 83.9 | 83.9 | 84.1 | 84.0 |

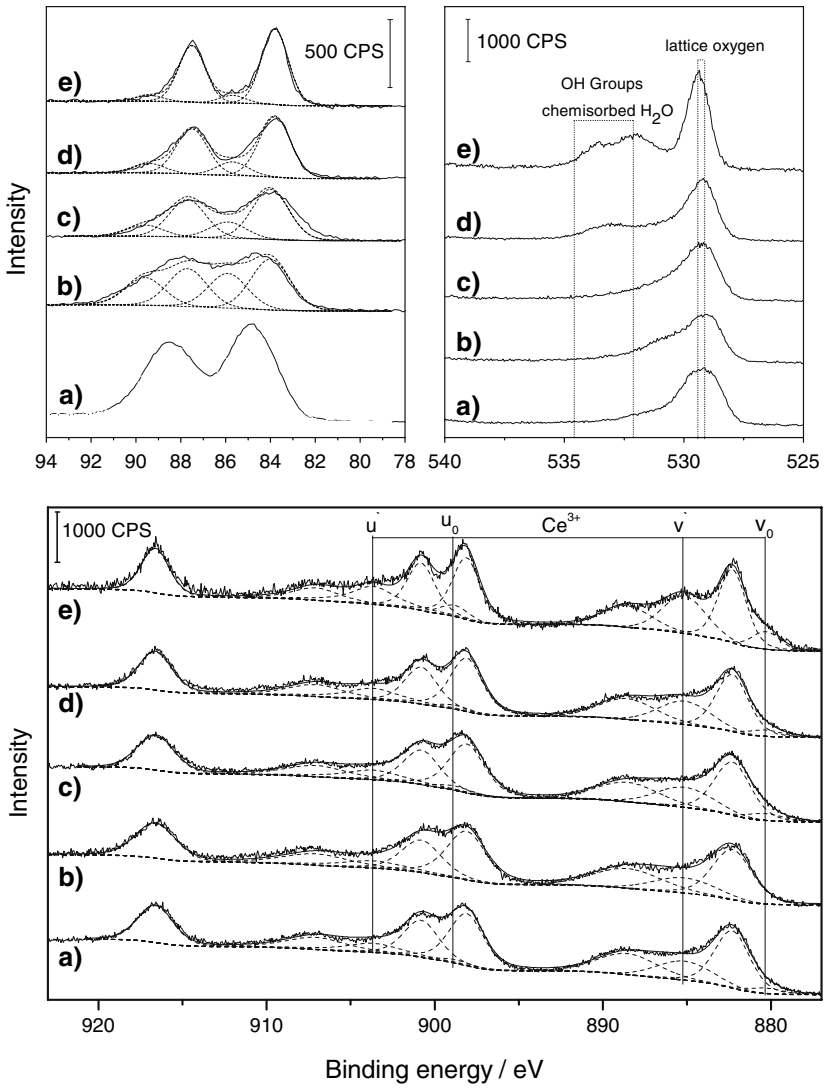


Figure 1. XP spectra of the Au(4f) region (left upper panel) of the Ce(3d) region (bottom panel) and of the O(1s) region (right upper panel) of an (a) untreated $Au/CeO_2$ (2.7 wt.% Au) pre-catalyst and after conditioning in (b) 10% $O_2/N_2$ at 200 °C, (c) 10% $O_2/N_2$ at 400 °C, (d) 10% $H_2/N_2$ at 200 °C and (e) 10% $H_2/N_2$ at 400 °C (parameters see text).

reductive treatment and with increasing temperature compared to the untreated $Au/CeO_2$ sample. In contrast, oxidative pre-treatment results in a decrease of the $Ce^{3+}$ amount after 200 °C calcination. After 400 °C calcination it increased slightly compared to the untreated sample, reaching values comparable to that of the *H200* sample.

Qualitatively, these results for Ce agree with our expectations and with trends observed for Au. For heating in $H_2$, thermal decomposition of $CeO_2$, and chemical reduction both work in the same direction, whereas for calcination these two processes (decomposition and chemical oxidation) are counteracting. Comparison with previous data also shows good agreement. Tabakova *et al.* [28] evaluated the $Ce^{3+}$ content of a $Au/CeO_2$ catalyst prepared via a modified deposition-precipitation procedure to 16% and 21% before and after reductive treatment at 150 °C in 1% $H_2/Ar$, respectively. Using a slightly different catalyst prepared via deposition-precipitation, they find no $Ce^{3+}$ on the 'as prepared' catalyst, but ~30% after reductive treatment in $H_2/Ar$ at 100 °C. For a similar type catalyst as used in the present study (2.7 wt.% $Au/CeO_2$) Leppelt *et al.* [23] reported a $Ce^{3+}$ concentration of 10% before reductive conditioning and ~22% after *H200* reductive treatment (table 1), and comparable amounts of $Ce^{3+}$ were reported also in ref. [25] for an almost identical catalyst after similar treatment. Jacobs *et al.* [43] showed an increase of the $Ce^{3+}$ amount to 19.2% in a 1 wt.% $Au/CeO_2$ catalyst during reductive treatment in $H_2/He$ (200 °C) using *in-situ* XANES (1 wt.% $Au/CeO_2$, 200 ccm $H_2$, 300 ccm He, 45 min), compared to about 23% $Ce^{3+}$ in a 1 wt.% $Pt/CeO_2$ catalyst after reduction at 250–350 °C. Romeo *et al.* [32] reported 17% $Ce^{3+}$ for their $Pd/CeO_2$ catalyst (2 wt.% Pd) after reduction at 400 °C. In total, reductive treatment of

noble metal/ceria catalysts at 200–400 °C results in $Ce^{3+}$ contents of 15–25%, with the exact value depending on the ceria particle size as well as respective reduction conditions.

Next, we used the $I_{Au(4f)}/I_{Ce(3d)}$ intensity ratio for an estimate of the trends in the Au particle size development, exploiting that for constant loading this value will decrease with increasing Au particle size because of the increasing Au(4f) absorption and the decreasing Ce(3d) absorption by the Au particles [44]. Clearly, this gains only qualitative information, but since the oxidative treatment results in particle sizes below the XRD detection limit, this at least gives qualitative information. The $I_{Au(4f)}/I_{Ce(3d)}$ intensity ratio decays in the order $RT > O200 > O400 > H200 = H400$ (table 1). This sequence follows the same order as that found for the $Au^0$ content, i.e., an increasing $Au^0$ content goes along with larger particle sizes. The increasing $Au^0$ content when going from the *H200* to the *H400* sample agrees also with the XRD observation of an increasing mean particle size for these samples (*H200*: 1.4 ± 0.4 nm, and *H400*: 2.6 ± 0.5 nm). In general, the presence of oxygen during the pre-treatment prevents the formation of larger $Au^0$ particles on ceria compared to reductive treatment.

XP spectra of the O(1s) region of differently treated $Au/CeO_2$ catalysts are presented in the right panel in figure 1 . For the untreated $Au/CeO_2$ catalyst we find a broad peak with a maximum between 529.0 and 529.6 eV and a small shoulder at 531.3 eV. These features are assigned to lattice oxygen and $OH_{ad}$ groups, respectively [39,45–49]. The area in the main peak at about 529.3 eV is about similar for all pre-treatment procedures (deviation < ±10%). The small variation can be explained by partial conversion of surface oxygen to OH groups, without significant variations in the total oxygen content. Calcination at 200 and 400 °C has no significant effect on the shape of the O(1s) signal. A small shift of the low energy 'lattice oxygen' peak maximum upon calcination can be explained as a result of (i) thermal decomposition of gold oxide [4], or (ii) decomposition of OH and carbonate species [18]. After reductive treatment at 200 and 400 °C, two additional peaks appear between 532 and 534 eV, which we attribute to OH groups and molecularly adsorbed water on the ceria support. This assignment, which follows interpretations of previous studies [47,49,50], agrees well with our DRIFTS results described below. They show a higher content of OH groups and chemisorbed water on the reduced catalysts compared to the calcined samples.

### 3.1.2. DRIFTS measurements

DRIFT spectra recorded on the untreated catalyst and after the different activation treatments at 180 °C (figure 2) reveal significant differences between the different catalysts. Most obvious are the differences in the OH-region. After reductive treatment (figure 2a, b) the

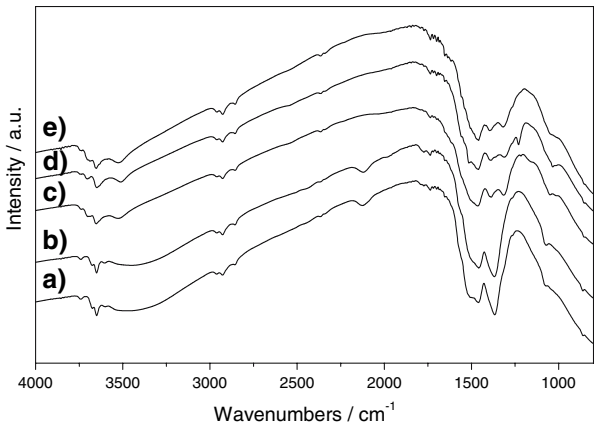


Figure 2. DRIFTS raw data of $Au/CeO_2$ after treatment in (a) 10% $H_2/N_2$ at 200 °C, (b) 10% $H_2/N_2$ at 400 °C, (c) 10% $O_2/N_2$ at 200 °C, (d) in 10% $O_2/N_2$ at 400 °C, (e) in $N_2$ at 200 °C (parameters see text).

spectra exhibit two peaks at 3649 and 3675 $cm^{-1}$, which are commonly assigned to bridged OH groups [43,51,52]. In addition, we find a broad peak at 3300–3500 $cm^{-1}$, characteristic for molecularly adsorbed water or hydrogen bonded OH groups on ceria [18,53,54]. After oxidative pre-treatment (figure 2c, d) as well as after drying in $N_2$ (figure 2e) these bridged OH groups are not observed, instead we find vibrational features at 3520, 3710 and 3655 $cm^{-1}$. Such signals had been attributed to linearly adsorbed (monodentate) and tridentate OH groups on ceria [46]. The broad 'water peak at 3300–3500 $cm^{-1}$ is not observed after these pre-treatments. In total, the DRIFT spectra confirm the XPS based conclusion of a strongly enhanced presence of molecularly adsorbed water after reductive treatment compared to calcination or drying in inert atmosphere. A similar correlation for the OH groups between both methods is not possible, since the strongly different background of the DRIFTS spectra renders a quantitative evaluation of the OH concentration impossible.

A peak at 2126 $cm^{-1}$, in the CO region, observed after reductive treatment is attributed to an electronic transition from donor levels located near the conduction band such as $Ce^{3+}$ or oxygen vacancies [53,55,56].

Independent of the conditioning procedure, carbonate species were clearly observed. After reductive pre-treatment of the $Au/CeO_2$ catalyst at 200 and 400 °C, three major peaks in the OCO-bending vibration region at 1511, 1462, 1367 $cm^{-1}$ (figure 2), respectively, provide unambiguous evidence for carbonates adsorbed on the ceria surface [57]. The first two peaks are observed also upon oxidation in $O_2$ at 200 and 400 °C, while the peak at 1367 $cm^{-1}$ is lower and split into two peaks at 1390 and 1310 $cm^{-1}$. Evidently, carbonates formed on the catalyst prior to the conditioning procedure are not destroyed during the pre-treatment. This interpretation agrees well with previous reports that temperatures up to 1000 °C are required to fully decompose carbonate species on ceria [58,59].

### 3.1.3. TPD measurements

Additional information on the presence of $OH_{ad}$ species and adsorbed water can be obtained by TPD experiments. Using the reduced *H200* catalyst as example, we investigated the presence of these species and their interaction with the catalyst by $O_2$ and $H_2O$-TPD. The spectra were recorded in a $N_2$ stream over pure ceria and over the $Au/CeO_2$ catalyst, after reductive pre-treatment in $H_2$ at 200 °C (figure 3). $O_2$ desorption from pure ceria (126 $\mu$mol) occurs in a peak centered at about 450 °C (upper panel, curve a). In contrast, on the $Au/CeO_2$ catalyst, $O_2$ desorption was essentially absent (upper panel, curve b). Apparently, the presence of gold drastically increases the efficiency of the reductive treatment for removing weakly bond oxygen from the ceria support. This was tested in $H_2O$-TPD experiments on similarly treated $CeO_2$ and $Au/CeO_2$ samples (figure 3, lower panel). The spectrum shows a sudden onset of $H_2O$ desorption at 270 °C, followed by a shoulder at 335 °C and two peaks with maxima at 425 and 565 °C, respectively for desorption from pure ceria (lower panel, curve a). These peaks can result either from desorption of molecularly adsorbed water or from recombination of adsorbed or bulk OH groups. For the $Au/CeO_2$ catalyst, $H_2O$ desorption is indeed much less pronounced, as expected from the higher tendency for $O_2$ desorption, which supports our above explanation. This result agrees well with observations of several authors, who showed an increasing tendency for ceria reduction at low temperature, in the presence of Au [26,43,60].

In total, these different spectroscopic measurements have clearly shown that

(i) the reductively treated samples have more OH groups than oxidatively treated $Au/CeO_2$ catalysts;
(ii) $Ce^{3+}$ defect sites are only created by reductive pre-treatment, while during oxidative treatment they are, depending on the temperature, more or less efficiently removed;
(iii) the presence of Au particles results in an enhanced reduction of $CeO_2$ during the reductive pre-treatment, equivalent to a more efficient removal of weakly bound oxygen;
(iv) pre-treatment in the temperature range between 200 and 400 °C does not fully remove carbon containing species such as carbonates from the $Au/CeO_2$ catalyst surface;
(v) reductive pre-treatment leads to larger particle sizes compared to oxidative pre-treatment.

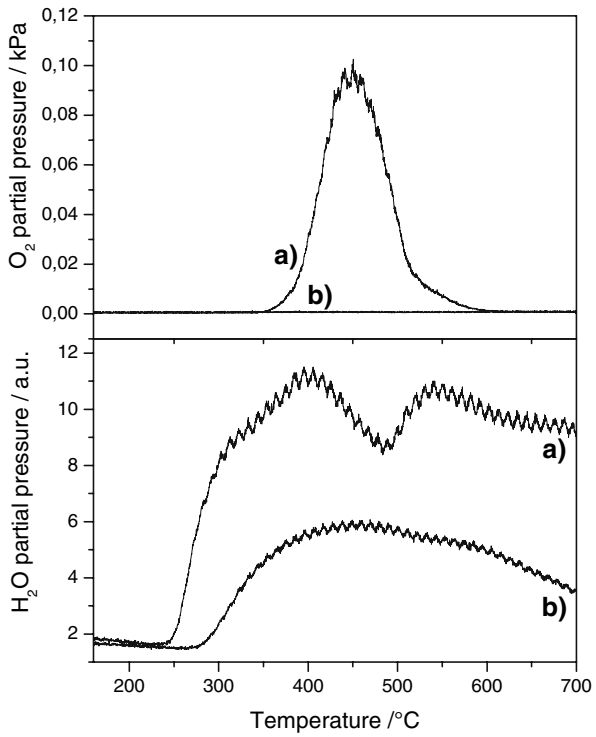


Figure 3. $O_2$-TPD (top panel) and $H_2O$-TPD (bottom panel) of (a) pure ceria and (b) a $Au/CeO_2$ catalyst after reductive pre-treatment at 200 °C, recorded in a $N_2$ stream (12 N ml $min^{-1}$, 5 °C $min^{-1}$).

### 3.2. Activity and stability of the $Au/CeO_2$ catalysts after different conditioning procedures

The evolution of the WGS reaction rate with time during reaction in idealized reformate on the differently pre-treated catalysts is illustrated in figure 4. Using the reaction rates after 1000 min for comparison, it is obvious from figure 4, that pre-treatment at 200 °C (a) *H200*, (b) *O200*, (c) *N200* results in significantly higher activities than conditioning at higher temperatures (curves (d–g) in figure 4). In contrast to the conditioning temperature, the effect of the conditioning atmosphere is less clear. While after conditioning at 200 and 300 °C, respectively, slightly higher reaction rates are obtained after reduction than after calcination, the rate is 2 times

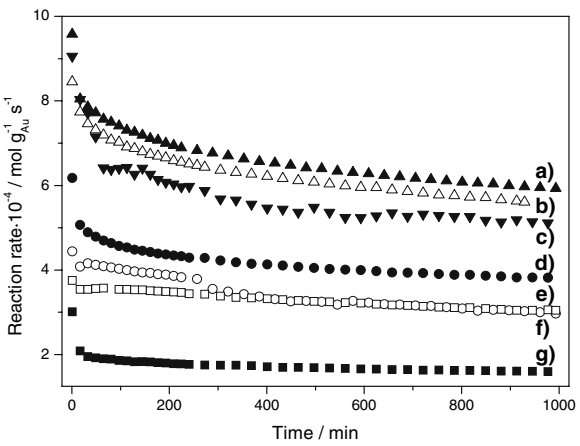


Figure 4. Initial activity and deactivation of differently pre-treated $Au/CeO_2$ catalysts in the WGS reaction in idealized reformate (1 kPa CO, 2 kPa $H_2O$, rest $N_2$) at 180 °C. Pre-treatment: (a) 200 °C in 10% $H_2/N_2$, (b) 200 °C in 10% $O_2/N_2$, (c) 200 °C in $N_2$, (d) 300 °C in 10% $H_2/N_2$, (e) 300 °C in 10% $O_2/N_2$, (f) 400 °C in 10% $O_2/N_2$ and (g) 400 °C in 10% $H_2/N_2$ (other parameters see text).

higher after calcination at 400 °C than after reduction at this temperature. The highest activity after 1000 min of reaction is obtained for the *H200* sample, after reductive pre-treatment at 200 °C.

Comparing these results with previously reported findings is almost impossible, since comparative studies on the effect of the conditioning process do not exist. In addition to varying the conditioning procedure or at least the conditioning parameters, also the procedure for catalyst preparation was changed, rendering quantitative conclusions on the effect of the conditioning procedure impossible. For instance, Tabakova *et al*. [28] compared two $Au/CeO_2$ catalysts with identical gold contents (3 wt.%), which were synthesized via deposition-precipitation (AuCeDP) and via a modified deposition-precipitation procedure (AuCeMDP). The samples were reduced in a 1% $H_2$/Ar atmosphere at different temperatures: the AuCeDP catalysts was reduced at 100 °C and the AuCeMDP sample at 150 °C. After these pre-treatments, the AuCeDP catalyst was by about a factor of five more active for reaction in a dilute $CO/H_2O$ mixture in Ar at 180 °C than the AuCeMDP sample. Hence, similar to our results reductive conditioning at lower temperatures results in a higher activity, but a preparation effect cannot be excluded, since the authors found a higher gold dispersion on the AuCeDP sample. Luengnaruemitchai *et al*. [14] reported a lower activity for a 1 wt.% $Au/CeO_2$ catalyst (preparation: coprecipitation) after oxidative treatment at 110 °C for 2 hours in $O_2$ than that determined by Andreeva *et al*. [26] for a similar loading catalyst (preparation: deposition-precipitation) after reduction at 100 °C in 1% $H_2$/Ar. A similar trend results also from measurements by Tabakova *et al*. [28] and Fu *et al*. [15] for 3 wt.% (2.6 at.%) and 4.5 at.% (5.1 wt.%) $Au/CeO_2$ catalysts, respectively.

Comparing the activities of the $Au/CeO_2$ catalysts obtained after the different conditioning procedures with previously reported activities of $Au/MeO_x$ and in particular $Au/CeO_2$ catalysts (see compilation of reaction data in table 2) shows that for comparable reaction conditions the catalysts prepared and investigated in this work are extremely active. They are clearly more active than the 400 °C calcined catalysts described by Fu *et al*. [15]. Sakurai *et al*. [9] studied the WGS reaction on various $Au/Me_xO_y$ catalysts and reported the following range of activity (see also table 2): $Au/TiO_2$ (3.4 at.%, DP) > $Au/Fe_2O_3$ (5 at.%, CP) > $Au/Al_3$ (5 at.%, CP) > Au/ZnO (5 at.%, CP). The reaction rate of the most active catalyst, $Au/TiO_2$, was 11 times lower than that of the $Au/CeO_2$ catalyst described in this study, after reductive pre-treatment. The apparently very high reaction rates reported in ref. [11] can be explained by the much higher CO and $H_2O$ contents; for a similar gas mixture we would obtain a rate of $135 \times 10^{-6}$ mol $g_{cat}^{-1}$ $s^{-1}$, using the reaction orders of 0.5 determined for both reactants in dilute water gas previously [23].

The stability of the $Au/CeO_2$ catalysts, as measured by the deactivation over 1000 min on-stream, also depends on the conditioning procedures (see figure 4 and table 3). Thermal treatment in inert atmosphere at 200 °C (*N200*) leads to the highest deactivation, while for reductive and oxidative conditioning at 200 and 300 °C, respectively, the deactivation is rather similar and significantly lower than for the *N200* sample. For conditioning at 400 °C, oxidative treatment (*O400*) results in a more stable catalyst; the deactivation is significantly lower than for all other samples, while reductive conditioning results in deactivation effects comparable to those at lower temperatures. Nevertheless, the absolute activity of the *O400* catalysts is significantly lower than that resulting after the other conditioning procedures.

Comparison of the present stability data with comparable data published previously shows a rather divergent situation. Luengnaruemitchai *et al*. [14] reported a dramatic decrease in conversion of their $Au/CeO_2$ (1 wt.% Au, BET 124.1 $m^2/g$) to approximately 37% of the initial activity in the course of 1000 min of reaction (2% CO, 20% $H_2O$, balance helium). Previous measurements in our group on $Au/CeO_2$ catalysts with

Table 2
Catalytic activity of supported gold catalysts for the WGS reaction

| Catalyst and metal loading (at.%) | Catalyst preparation | BET ($m^2$ $g^{-1}$) | Reaction temp. (°C) | Reaction atmosphere | Rate $\times 10^6$ (mol $g_{cat}^{-1}$ $s^{-1}$) | Reference |
|---|---|---|---|---|---|---|
| 3.8% $Au/CeO_2$ | CP | 71.8 | 175 | 1% CO, 2% $H_2O$ in $N_2$ | 2.2 | [15] |
| 4.5% $Au/CeO_2$ | DP | 155.8 | 175 | 1% CO, 2% $H_2O$ in $N_2$ | 3.4 | [15] |
| 4.7% $Au/CeO_2$ | DP | 82.7 | 175 | 1% CO, 2% $H_2O$ in $N_2$ | 1.4 | [15] |
| 2.3% $Au/CeO_2$ (2.7 wt.%) | DP | 188 | 180 | 1% CO, 2% $H_2O$ in $N_2$ | 11 | [23] |
| 2.4% $Au/CeO_2$ (2.7 wt.%) | DP | 188 | 180 | 1% CO, 2% $H_2O$ in $N_2$ | 16 | Here |
| 3.4% $Au/TiO_2$ | DP | | 180 | 1% CO, 2% $H_2O$ in He | 1.4 | [9] |
| 5% Au/ZnO | CP | | 180 | 1% CO, 2% $H_2O$ in He | 0.06 | [9] |
| 5% $Au/Al_2O_3$ | CP | | 180 | 1% CO, 2% $H_2O$ in He | 0.13 | [9] |
| 5% $Au/Fe_2O_3$ | CP | | 180 | 1% CO, 2% $H_2O$ in He | 0.43 | [9] |
| 4.3% $Au/Fe_2O_3$ | CP | 20 | 180 | 4.88% CO, 29.3% $H_2O$ | 178 | [11] |
| 3% $Au/Fe_2O_3$ | DP | | 240 | 5.9% CO, 94.1% $H_2O$ | 0.35 | [61,62] |

DP – Deposition-precipitation; CP – coprecipitation; UGC – urea gelation/coprecipitation.

Table 3
Deactivation of a 2.7 wt.% $Au/CeO_2$ catalyst during 1000 min WGS reaction in dilute water gas at 180 °C after different conditioning procedures (details see text)

| Pre-treatment temperature (°C) | 200 | 300 | 400 |
|---|---|---|---|
| Reductive pre-treatment | *H200* | *H300* | *H400* |
| Deactivation (%) | 26.3 | 24.6 | 23.3 |
| Oxidative pre-treatment | *O200* | *O300* | *O400* |
| Deactivation (%) | 27.6 | 27.6 | 14.1 |
| Thermal pre-treatment | *N200* | | |
| Deactivation (%) | 36.2 | – | – |

gold contents between 0.8 and 12.6 wt.% led to results comparable to those of the present study (reductive conditioning, deactivation by $20 \pm 5\%$ of the initial activity over 1000 min) [23]. Andreeva *et al*. [26], on the other hand, reported about very stable $Au/CeO_2$ catalysts (content 3 wt.% of gold), whose final activity exceeded the initial conversion after 3 weeks of operation. Furthermore they also observed a decreasing Au particle size, from initially rather large particles (5.5 nm diameter) towards smaller ones.

In total, the reaction measurements clearly demonstrate that reductive conditioning (reduction at 200 °C, *H200*) represents the optimum conditioning procedure for the deposition-precipitation prepared $Au/CeO_2$ catalysts investigated in this study.

### 3.3. *Influence of the conditioning procedure on the adlayer evolution during reaction in idealized reformate (DRIFTS)*

The accumulation of adsorbed reaction intermediates and side products on the differentially conditioned catalysts was followed by *in-situ* IR spectroscopy (DRIFTS) measurements. Sequences of spectra recorded during 1000 min on-stream, under similar conditions as applied for the kinetic measurements, are displayed in figure 5. Full spectra are shown in the bottom panel, expanded representations of the O–H region, of the C–H region and of the $CO_2$/CO region are presented in the upper left and upper right panel, respectively, for each catalyst. On all four catalysts three formate peaks at 1587, 1372 and 2836 $cm^{-1}$ develop. The first two peaks are related to asymmetric and symmetric O–C–O modes of bidentate formate species [18,56,63]. The band at 2836 $cm^{-1}$ can be assigned to the C–H vibration stretching mode of bidentate formate species [51,52,64]. The other peak in the C–H region, located at 2949 $cm^{-1}$, results from bridged formate [18,51,64] on ceria. For all catalysts we find the characteristic 1420 $cm^{-1}$ band of monodentate carbonate increasing with time. In a previous study we had identified this species as mainly responsible for the deactivation of the catalysts during the WGS reaction [24]. After oxidative conditioning we find an additional 'carbonate' species characterized by a peak at 1372 $cm^{-1}$ [51–55,57], which can be distinguished from bidentate formate species by the fact that the time dependent variation of the related C–H vibration (2836 $cm^{-1}$) is much less pronounced.

The two peaks at 2336 and 2362 $cm^{-1}$ result from gas phase $CO_2$, which is produced by the WGS reaction on $Au/CeO_2$. They decay with time, both the decay with time as well as the initial and final intensity depend on the conditioning procedure. Comparison of the intensities of the $CO_2$ signals and their variation with time with the $CO_2$ formation rates after the different conditioning procedures (figure 4) yields qualitative agreement between these quantities, both for the absolute intensities and for the decay with time.

Also for the OH groups we see distinct differences and changes with time, where the main changes occurred during the first few minutes. For the reduced catalysts, the "water" peak at 3300–3500 $cm^{-1}$ disappeared. The intensity of the bridged OH group at 3649 $cm^{-1}$ [23,52,65] decreased strongly, and a new peak at 3630 $cm^{-1}$ appeared. A peak at 3600 $cm^{-1}$ (see ref. [23]) shifted to 3590 $cm^{-1}$. Only small changes occurred for the second type of bridged OH groups (3675 $cm^{-1}$). On the oxidized $Au/CeO_2$ catalyst, where after the pre-treatment the OH groups differed significantly from those observed on reduced catalysts (see section 3.1), the same OH group related signals developed during the reaction. Already after 10 min WGS reaction, no difference in the OH groups is observed between reduced or oxidized $Au/CeO_2$ catalysts. This finding leads to the suggestion that the initially different catalyst surfaces develop towards the same surface composition, at least with respect to the different types of surface sites. Quantitatively, however, there are still distinct differences. In the case of the reductively conditioned $Au/CeO_2$ catalyst more bridged bond OH groups at 3649 $cm^{-1}$ are present after conditioning and also after 1000 min on stream, although after that reaction time the difference to the oxidatively conditioned catalyst is less strong. Obviously, 1000 min reaction time is not sufficient to reach similar steady-state surface composition for the differently pre-treated catalysts.

The IR-data presented above are compatible with the mechanism we had recently proposed for the WGS reaction on $Au/CeO_2$ catalysts, for the dominant reaction pathway [23], which involves the reaction of $CO_{ad}$ with OH groups to form adsorbates formates, which can migrate on the ceria substrate and return to the active sites to decompose into $CO_2$ and $H_2$. For present reaction conditions, decomposition of bidentate formates was determined as rate limiting step, although under steady-state conditions, formate formation must be equally fast as formate decomposition. In that mechanism, the ceria surface acts as buffer for adsorbed formate species, which can be considered as stable reaction intermediates. Independent of the pre-treatment, we found the same type of bidentate formates on all

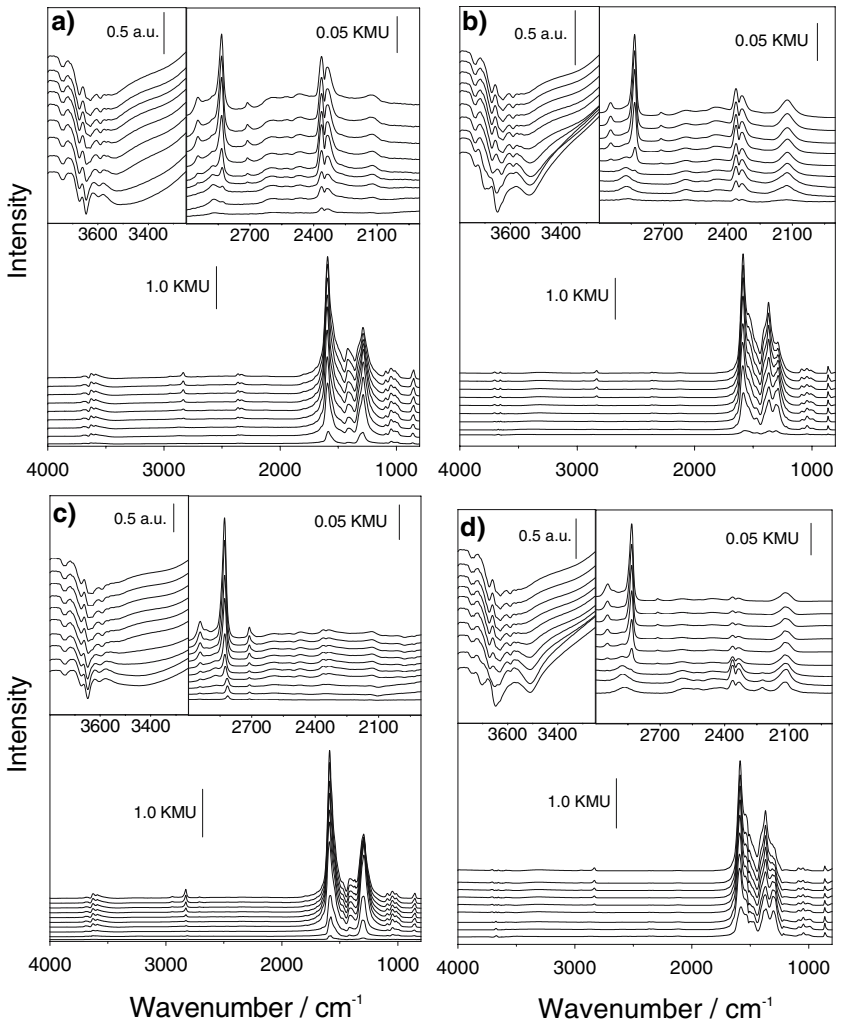


Figure 5. Series of DRIFT spectra obtained during the WGS reaction in idealized reformate (dilute water gas, 0.5 kPa CO, 1 kPa $H_2O$, the rest $N_2$) over 1000 min on $Au/CeO_2$ catalysts pre-treated at 200 °C in (a) 10% $H_2/N_2$ and (b) 10% $O_2/N_2$ and at 400 °C in (c) 10% $H_2/N_2$ and (d) 10% $O_2/N_2$. Bottom: full spectrum, top left: detail spectra of the O–H region (raw data), top right detail spectra of the C–H region; from bottom to top after 23 s, 35 s, 47 s, 2 min, 4 min, 10 min, 30 min, 60 min, 240 min, 1000 min.

catalysts, indicating that the general reaction mechanism is not altered by the different pre-treatment procedure. The highest formate content is observed for the *H400* pre-treated sample, it is lower for *O400* and *O200* catalysts, and lowest on the *H200* catalyst. This trend is opposite to the change of the $CO_2$ production rate with pre-treatment. Apparently, on the *H200* catalyst the formate decomposition rate, which is identical to the $CO_2$ formation rate, is highest. This results in the lowest steady-state content of active, bidentate formates.

On the other hand, under steady-state conditions the higher rate for formate decomposition must be supported also by a higher rate for formate formation. Differences in the formate formation rate seem to be correlated with the abundance of bridged OH groups on the surface, which is highest on the reductively pre-treated *H200* catalyst, slightly lower for the *H400* and significantly lower for the oxidatively pre-treated catalysts.

In that way, the pre-treatment is important since it affects both the bidentate formate decomposition rate and the formate formation rate as rate limiting steps in the WGS reaction [23]. The physical origin for the different rates for formate formation and decomposition must lie in the different $Ce^{3+}$ and the $Au^{n+}$ contents and in the different $Au^0$ particle sizes. (The influence of a varying $CeO_2$ particle size, which was kept constant in the present study, was investigated in ref. [25].) However, there is no clear trend which would identify one of these properties as the only decisive one.

Comparing the variation of the $Au^0$ amounts in the differently conditioned samples (see table 1) with that in the activity measurements, there is no clear correlation between these two properties. On the other hand, also the $Au^{3+}$ content is not directly correlated with the activity, since the *H200* and *O400* catalysts have about the same $Au^{3+}$ content, while the reaction rate was about twice as high for the *H200* catalysts as for the *O400* sample. This

result appears to be in contrast to the conclusion by Fu *et al.* [15,19], who proposed that the WGS activity is dominated by $Au^{+}$ species and that $Au^{0}$ only acts as a spectator. One should keep in mind, however, that their studies were performed on 400 °C calcined catalysts, which based on the present findings are considerably less active than the reductively pre-treated catalysts, and that they proposed a $Au^{1+}$ species as active species (XPS BE: $Au^{1+}$(4f): 84.6 eV, $Au^{3+}$(4f): 85.9 eV), while the $Au^{n+}$ species in the present study mainly refer to the $Au^{3+}$ species characterized by a Au($4f_{7/2}$) BE of 85.8 eV. The variation in the Au particle size does follow the trend of the activity for the reductively pre-treated catalysts, but not when comparing with the oxidatively pre-treated catalysts. Also the $Ce^{3+}$ content shows no clear correlation with the measured WGS activity, although previous reports demonstrated a significant role of the $Ce^{3+}$ content in the WGS reaction [28,48,60,66]. The *H400* sample, which has the lowest activity by far, has a significantly higher amount of $Ce^{3+}$, compared to the other samples, while on the other hand the most active *H200* sample has a significantly higher $Ce^{3+}$ content than the (less active) oxidatively pre-treated catalysts. Comparison of the *H200* and *O200* catalysts shows little difference in activity, but significant differences in the $Ce^{3+}$ content (14% versus 21%)

Based on these data we conclude that there is not a single effect or quantity determining the WGS activity of $Au/CeO_2$ catalysts, but that this results from an interplay of different quantities such as the abundance of ionic $Ce^{3+}$ and $Au^{n+}$ species as well as the $Au^{0}$ and ceria particle sizes and that these will affect the concentration of active reactants such as bridged OH groups as well as that of stable reaction intermediates such as bidentate formate. This result is not at all astonishing, since under steady-state conditions both formate formation as well as formate decomposition are equally important for the WGS activity, and the above quantities will affect the rates for these two reactions in a different way. In that sense, the most active catalyst is characterized by a high activity for formate formation *and* a high activity for formate decomposition, where the former seems to be correlated to a high abundance of bridged OH groups and the latter rate is dominated by the activity and abundance of active sites for formate decomposition and by the transport to these sites (see ref. [23]). These rates are likely to rely in different ways on the surface composition characterized by the content of $Au^{n+}$ and $Ce^{3+}$ and the respective particle of sizes, i.e., they are affected by different properties of the catalyst surface. The interplay between these two rates determines the amount of active (bidentate) formate species stored on the ceria surface. In that sense, the overall surface composition of the reductively pre-treated *H200* catalyst seems to be optimal for achieving high rates for formate formation and formate decomposition at the same time.

## 4. Conclusion

We have investigated the influence of the conditioning procedure on the surface composition, activity and stability of 2.7 wt.% $Au/CeO_2$ catalysts prepared by a deposition-precipitation procedure, comparing conditioning in inert, oxidative and reductive atmosphere at temperatures between 200 and 400 °C. Based on *ex-situ* (XPS) and *in-situ* (DRIFTS) spectroscopic and on kinetic measurements we could demonstrate that the conditioning procedure has significant influence on the surface composition, activity and stability of these catalysts. Comparing activities after 1000 min on stream, the optimum conditioning procedure involves reduction in 10% $H_2/N_2$ at 200 °C (45 min). The resulting catalysts are highly active also in comparison with data reported previously.

The catalyst activity drops with increasing pre-treatment temperature. The comparison of reductive and oxidative pre-treatments shows a higher activity for the reductively conditioned catalysts, except for the high temperature (400 °C) conditioned *H400* catalysts, which turned out to have the lowest activity. The tendency for deactivation drops slightly with increasing conditioning temperature, except for the *O400* catalyst, which shows a pronounced decay in deactivation, from about 25–26% at 200 and 300 °C to 14% after 400 °C calcination.

The spectroscopic measurements show that the activity is correlated with the abundance of bridged OH groups, which can react with CO to form adsorbed formates, and inversely correlated with the concentration of bidentate formate species, supporting our previous proposal that on these catalysts the WGS reaction proceeds via the formation and decomposition of adsorbed formates and that the ceria surface acts as storage for adsorbed formates. The fact that there is no clear correlation between any of the three properties $Au^{3+}$ content, $Ce^{3+}$ content and $Au^{0}$ particle size and the WGS activity is interpreted in a way that none of these properties is solely decisive for the WGS activity, but that they affect in different ways the activities (rates) for formate formation and formate decomposition. Under steady-state conditions the two rates together determine the measured WGS rate and, via the ratio of the respective rate constants, the steady-state coverage of the bidentate formate intermediate. Accordingly, the most active *H200* catalyst is characterized by a combination of these properties which is optimal for enhancing both formate formation and formate decomposition.

## Acknowledgments

We gratefully acknowledge financial support by the Deutsche Forschungsgemeinschaft, via Research Training Group 328 (“Molecular Organization and Dynamics at Interfaces and Surfaces”) and via project Be 1201/9-4.

## References


[1] M. Haruta, N. Yamada, T. Kobayashi and S. Iijima, J. Catal. 115 (1989) 301.
[2] G.C. Bond and D.T. Thompson, Gold Bull. 34 (2000) 117.
[3] D. Andreeva, Gold Bull. 35 (2002) 82.
[4] M. Haruta, S. Tsubota, T. Kobayashi, H. Kageyama, M.J. Genet and B. Delmon, J. Catal. 144 (1993) 175.
[5] R. Kumar and S. Ahmed, in: *Fuels processing for transportation fuel cell systems*, eds. O. Savadogo, P.R. Roberge and T.N. Veziroglu (Les Éditions de l'École Polytechnique de Montréal, Montréal, Québec, Canada, 1995), pp. 224–238.
[6] D.L. Trimm and Z.I. Önsan, Catal. Rev. 43 (2001) 31.
[7] T. Tabakova, V. Idakiev, D. Andreeva and I. Mitov, Appl. Catal. A 202 (2000) 91.
[8] L.I. Ilieva, G. Munteanu and D.C. Andreeva, Bulg. Chem. Comm. 30 (1998) 378.
[9] H. Sakurai, A. Ueda, T. Kobayashi and M. Haruta, Chem. Commun. (1997) 271.
[10] F. Boccuzzi, A. Chiorino, M. Manzoli, D. Andreeva and T. Tabakova, J. Catal. 188 (1999) 176.
[11] D. Andreeva, V. Idakiev, T. Tabakova, A. Andreev and R. Giovanoli, Appl. Catal. A 134 (1996) 275.
[12] D. Andreeva, V. Idakiev, T. Tabakova and A. Andreev, J. Catal. 158 (1996) 354.
[13] D. Andreeva, T. Tabakova, V. Idakiev, P. Christov and R. Giovanoli, Appl. Catal. A 169 (1998) 9.
[14] A. Luengnaruemitchai, S. Osuwan and E. Gulari, Catal. Commun. 4 (2003) 215.
[15] Q. Fu, A. Weber and M. Flytzani-Stephanopoulos, Catal. Lett. 77 (2001) 87.
[16] H. Sakurai, T. Akita, S. Tsubota, M. Kiuchi and M. Haruta, Appl. Catal. A 291 (2005) 179.
[17] W. Deng, J. De Jesus, H. Saltsburg and M. Flytzani-Stephanopoulos, Appl. Catal. A 291 (2005) 126.
[18] T. Tabakova, F. Boccuzzi, M. Manzoli and D. Andreeva, Appl. Catal. A 252 (2003) 385.
[19] Q. Fu, H. Saltsburg and M. Flytzani-Stephanopoulos, Science 301 (2003) 935.
[20] Q. Fu, W. Deng, H. Saltsburg and M. Flytzani-Stephanopoulos, Appl. Catal. B 56 (2005) 57.
[21] B. Schumacher, V. Plzak, M. Kinne and R.J. Behm, Catal. Lett. 89 (2003) 109.
[22] V. Plzak, J. Garche and R.J. Behm, Eur. Fuel Cell News 10 (2003) 16.
[23] R. Leppelt, B. Schumacher, V. Plzak, M. Kinne and R.J. Behm, J. Catal. 244 (2006) 137.
[24] Y. Denkwitz, A. Karpenko, V. Plzak, R. Leppelt, B. Schumacher and R.J. Behm, J. Catal. 246 (2007) 74.
[25] A. Karpenko, R. Leppelt, V. Plzak, J. Cai, A. Chuvilin, B. Schumacher, U. Kaiser and R.J. Behm, Topics Catal. (in press).
[26] D. Andreeva, V. Idakiev, T. Tabakova, L. Ilieva, P. Falaras, A. Bourlinos and A. Travlos, Catal. Today 72 (2002) 51.
[27] C.H. Kim and L.T. Thompson, J. Catal. 230 (2005) 66.
[28] T. Tabakova, F. Boccuzzi, M. Manzoli, J.W. Sobczak, V. Idakiev and D. Andreeva, Appl. Catal. B 49 (2004) 73.
[29] A.M. Visco, F. Neri, G. Neri, A. Donato, C. Milone and S. Galvagno, Phys. Chem. Chem. Phys. 1 (1999) 2869.
[30] S.T. Daniells, A.R. Overweg, M. Makkee and J.A. Moulijn, J. Catal. 230 (2005) 52.
[31] N.A. Hodge, C.J. Kiely, R. Whyman, M.R.H. Siddiqui, G.J. Hutchings, Q.A. Pankhurst, F.E. Wagner, R.R. Rajaram and S.E. Golunski, Catal. Today 72 (2002) 133.
[32] M. Romeo, K. Bak, J. El Fallah, F. Le Normand and L. Hilaire, Surf. Interf. Anal. 20 (1993) 508.
[33] D. Briggs and M.P. Seah, *Practical Surface Analysis – Auger and X-Ray Photoelectron Spectroscopy*, 2nd ed. (John Wiley & Sons, Chichester, 1990).
[34] F. Zhang, P. Wang, J. Koberstein, S. Khalid and S.-W. Chan, Surf. Sci. 563 (2004) 74.
[35] P.B. Weisz, Chem. Eng. Progr. Symp. Ser. 55 (1992) 29.
[36] M.J. Kahlich, H.A. Gasteiger and R.J. Behm, J. Catal. 171 (1997) 93.
[37] I.M. Hamadeh and P.R. Griffiths, Appl. Spec. 41 (1987) 682.
[38] M.M. Schubert, M.J. Kahlich, H.A. Gasteiger and R.J. Behm, J. Power Sources 84 (1999) 175.
[39] J.-J. Pireaux, M. Liehr, P.A. Thiry, J.P. Delrue and R. Caudano, Surf. Sci. 141 (1984) 21.
[40] J.F. Moulder, W.F. Stickle, P.E. Sobol and K.D. Bomben, *Handbook of X-ray Photoelectron Spectroscopy* (Perkin Elmer Corp., Eden Prairie/USA, 1992).
[41] H.-G. Boyen, G. Kästle, F. Weigl, B. Koslowski, C. Dietrich, P. Ziemann, J.P. Spatz, S. Riethmüller, C. Hartmann, M. Möller, G. Schmid, M.G. Garnier and P. Oelhafen, Science 297 (2002) 1533.
[42] Q. Fu, S. Kudriavtseva, H. Saltsburg and M. Flytzani-Stephanopoulos, Chem. Eng. J. 93 (2003) 41.
[43] G. Jacobs, P.M. Patterson, L. Williams, E. Chenu, D. Sparks, G. Thomas and B.H. Davis, Appl. Catal. A 262 (2004) 177.
[44] J.W. Niemantsverdriet, *Spectroscopy in Catalysis – An Introduction* (VCH).
[45] T. Dickinson, A.F. Povey and P.M.A. Sherwood, J. Chem. Soc. Faraday Trans. 71 (1974) 298.
[46] A. Laachir, V. Perrichon, A. Badri, J. Lamotte, E. Catherine and J.C. Lavalley, J. Chem. Soc. Faraday Trans. 87 (1991) 1601.
[47] G.S. Herman, Y.J. Kim, S.A. Chambers and C.H.F. Peden, Langmuir 15 (1999) 3993.
[48] Lj. Kundakovic, D.R. Mullins and S.H. Overbury, Surf. Sci. 457 (2000) 51.
[49] M.M. Natile, G. Boccaletti and A. Glisenti, Chem. Mater. 17 (2005) 6272.
[50] D.R. Mullins, S.H. Overbury and D.R. Huntley, Surf. Sci. 409 (1998) 307.
[51] T. Shido and Y. Iwasawa, J. Catal. 136 (1992) 493.
[52] T. Shido and Y. Iwasawa, J. Catal. 141 (1993) 71.
[53] C. Binet, A. Badri and J.C. Lavalley, J. Phys. Chem. 98 (1994) 6392.
[54] C. Binet, M. Daturi and J.-C. Lavalley, Catal. Today 50 (1999) 207.
[55] F. Bozon-Verduraz and A. Bensalem, J. Chem. Soc. Faraday Trans. 90 (1994) 653.
[56] E. Finocchio, M. Daturi, C. Binet, J.C. Lavalley and G. Blanchard, Catal. Today 52 (1999) 53.
[57] C. Li, Y. Sakata, T. Arai, K. Domen, K. Maruya and T. Onishi, J. Chem. Soc. Faraday Trans. 85 (1989) 929.
[58] T. Mokkelbost, I. Kaus, T. Grande and M.A. Einarsrud, Chem. Mater. 16 (2004) 5489.
[59] A. Bumajdad, M.I. Zaki, J. Eastoe and L. Pasupulety, Langmuir 20 (2004) 11223.
[60] A. Trovarelli, Catal. Rev. Sci. Eng. 38 (1996) 439.
[61] A. Venugopal and M.S. Scurrell, Appl. Catal. A 245 (2003) 137.
[62] A. Venugopal, J. Aluha, D. Mogano and M.S. Scurrell, Appl. Catal. A 245 (2003) 149.
[63] C. Li, Y. Sakata, T. Arai, K. Domen, K. Maruya and T. Onishi, J. Chem. Soc. Faraday Trans. 85 (1989) 1451.
[64] G. Jacobs, L. Williams, U. Graham, D. Sparks and B.H. Davis, J. Phys. Chem. B 107 (2003) 10398.
[65] G. Jacobs, L. Williams, U. Graham, G.A. Thomas, D.E. Sparks and B.H. Davis, Appl. Catal. 252 (2003) 107.
[66] Z.-W. Liu, Q.-H. Wei and X. Zhang, Nano Lett. 5 (2005) 957.